

## CONTROL OF SPACE PLATFORMS WITH FLEXIBLE LINKS USING COMMAND SHAPING METHOD\*

A. EBRAHIMI, S. A. A. MOOSAVIAN\*\* AND M. MIRSHAMS

Dept. of Mechanical Engineering K.N .Toosi University of Technology  
Tehran, Iran, P.O. Box 19395-1999, Fax: (+98) 21 8867-4748  
Email: Moosavian@kntu.ac.ir

**Abstract**– The rapid growth of space utilization requires construction and maintenance of space structures and satellites in orbit that, in turn, substantiate the application of robotic systems in space. In this paper, a near-minimum-time optimal control law is developed for a rigid space platform with flexible links such as manipulators, solar panels and stabilizing booms during an orientating maneuver with a large angle of rotation. The time optimal control solution for the rigid-body mode is obtained as a bang-bang function and applied to the flexible system after smoothing the control inputs to avoid stimulation of the flexible modes. This will also reflect practical limitations in exerting bang-bang actuator forces/torques, due to delays and non-zero time constants of existing actuation elements. The smoothness of the input command is obtained by reshaping its profile based on consideration of additional derivative constraints. The platform is modeled as a linear undamped elastic system that yields an appropriate model for the analysis of planar rotational maneuvers. The developed control law is applied on a given satellite during a slewing maneuver, and the simulation results show that the modified realistic optimal input compared to the bang-bang solution goes well with the practical limitations and also alleviates the vibrating motion of the flexible appendage, which reveals the merits of the new developed control law.

**Keywords**– Slewing spacecraft, flexible links, space robots, optimal control, command shaping

### 1. INTRODUCTION

Extending the life of space systems, and therefore reducing the associated costs, will require extensive inspection, assembly and maintenance capabilities in orbit. Therefore, it is expected that robotic devices will play a more important role in future missions, [1]. In order to control such systems, it is essential to develop a proper kinematics/dynamics model for the system that has been studied under the assumption of rigid elements [2-5], and elastic elements [6-8]. There have also been various studies on the nonlinear control problem of such systems with both rigid and flexible elements, [9-14].

Tackling time limitations in space rendezvous, the optimal control with a time minimization constraint is of main importance. It should be noted that high speeds, in turn, might stimulate the system flexible modes, which could drastically affect the control system performance. Space projects involving large structures, satellites with antennas or solar panels, stabilizing boom, and robotic manipulators are examples where one should consider achieving rapid maneuvers without stimulating flexible modes. Therefore, the minimum-time optimal control for the rigid mode and  $n$  flexible modes has become the focus of several articles, [15-17]. The time-optimal controller is obtained by solving the state and co-state equations, considering Pontryagin's minimum principle. The bang-bang type of control causes spillover

\*Received by the editors February 14, 2005; final revised form November 21, 2007.

\*\*Corresponding author

effects that may induce high residual flexural energy due to instantaneous switching in actuating forces/torques. Using an approximation routine for the bang-bang input with the objective of eliminating the sudden changes at switching times, a smoother control input can be obtained, [18-19], where a near minimum time optimal solution is obtained based on constrained Pontryagin's principle. While in a real implementation this is of great importance, unfortunately this approach is not able to thoroughly shape the input based on realistic actuation capabilities.

In this paper, to suppress and ideally eliminate the vibration of elastic appendages of a space platform, a preshaping method is presented which results in a near minimum time optimal controller. Therefore, the optimal control problem is solved by constrained parameters optimization, which yields directly switching times. To this end, a near-minimum-time optimal control law for a rigid space platform with flexible links during an orientating maneuver with a large angle of rotation is developed. The time optimal control solution for the rigid-body mode is obtained as a bang-bang function. The obtained control law is applied to the flexible system after smoothing the control inputs to reflect practical limitations in exerting bang-bang actuator forces/torques. The smoothness of the input command is obtained by reshaping its profile with the first and second time derivatives constraints. The assumed modes method for the flexible appendage will be used where the Euler-Bernoulli beam model is adopted. Based on the obtained smooth control functions, the switching times are obtained by *converting* the optimal control problem into a constrained parameters optimization problem which will be solved numerically. The developed control law is applied on a given satellite which consists of two elastic panels, during a slewing maneuver. The first five flexible modes are considered in the simulated model, whereas a single torque actuator is located on the central rigid body. The task is to rotate the system by a certain angular displacement in minimum time. The simulation results show that the developed realistic optimal input compared to the bang-bang solution goes well with the practical limitations and can successfully control the end-point motion of the flexible appendages.

## 2. EQUATIONS OF MOTION

In this section, the dynamics of the slewing flexible spacecraft is investigated. The assumed modes method for the flexible appendage will be used, with no structural damping, where the Euler-Bernoulli beam model is adopted. The control actuator is modeled as a torque generating device,  $\mathbf{u}(t)$ , acting on the main body. Since the slewing maneuver is of relatively short length and duration, microgravity and dynamical effects due to orbital mechanics are negligible, compared to the control torque. Considering a rigid central body rotating in inertial space, with flexible appendages, it is assumed that the flexible beam performs only planar motion as shown in Fig. 1. Frames  $(X_1 X_2 X_3)$  and  $(x_1 x_2 x_3)$  denote an inertial (orbital) frame and a body-fixed coordinate, where  $(\hat{X}_1, \hat{X}_2, \hat{X}_3)$  and  $(\hat{x}_1, \hat{x}_2, \hat{x}_3)$  are unit vectors of these frames, respectively. The origins of both frames (O) are located at the center of the mass of the main rigid body, and  $x_1, x_2, x_3$  are defined along the principal axes of the rigid body. The flexible beam is clamped to the rigid body at point C, and  $\theta$  is the angle of rotation of the rigid body. (see Fig.1).

The governing differential equations of motion can be obtained from the extended Hamilton's principle [20], described as

$$\int_{t_0}^{t_1} (\delta L + \delta W) dt = 0 \quad (1.1)$$

where L represents the system Lagrangian as a difference between the system kinetic energy ( $\mathbf{T}$ ) and potential energy ( $\mathbf{V}$ )

$$L = \mathbf{T} - \mathbf{V} \quad (1.2)$$

and  $\delta W$  is the virtual work done by the control torque  $\mathbf{u}(t)$

$$\delta W = \delta\theta \mathbf{u}(t) \quad (2)$$

where  $\delta\theta$  is angular displacement due to control torque  $\mathbf{u}(t)$ . Assuming Euler Bernoulli beam theory and small deformation, the total kinetic energy of the system contains two terms corresponding to the central body and the appendages which can be written as:

$$T = \frac{1}{2} I_3 \dot{\theta}^2 + \frac{1}{2} \int_0^L \rho \bar{V} \cdot \bar{V} dx \quad (3)$$

where  $x$  defines the position of any point of an appendage with respect to point C,  $I_3$  is the inertia of the rigid body along the  $\mathbf{x}_3$  axis,  $\dot{\theta}$  is the angular velocity of the spacecraft,  $L$  is the length of the appendages,  $\rho$  is the mass per unit length of the appendages, and  $\bar{V}$  defines the velocity of any point of the appendage which can be obtained as

$$\bar{V}(x, t) = \dot{\bar{r}} = \dot{\bar{r}}_B + \bar{\omega} \times \bar{r} \quad (4)$$

where  $\dot{\bar{r}}_N$  and  $\dot{\bar{r}}_B$  denote the velocity in the inertial and body-fixed reference frames, respectively.  $\bar{\omega} = \dot{\theta} \hat{x}_3$  is the angular velocity of the main rigid body which is equal to its body-fixed frame angular velocity with respect to orbital frame, and  $\bar{r}$  defines the position vector of any point of the appendage which can be expressed as

$$\bar{r}(x, t) = (b + x) \hat{x}_1 + y \hat{x}_2 \quad (5)$$

where  $y(x, t)$  is the elastic deformation (the lateral displacement) of the appendage at time  $t$  and distance  $x$ , and  $b$  is the distance between the system center of mass to the point of attachment (C). Substituting Eq. (5) into Eq. (4) we obtain

$$\bar{V}(x, t) = -\dot{\theta} \hat{x}_1 + [(b + x)\dot{\theta} + \dot{y}] \hat{x}_2 \quad (6)$$

Substituting Eq. (6) into Eq. (3) leads to:

$$T = \frac{1}{2} \bar{I} \dot{\theta}^2 + \rho \int_0^L \dot{y}^2 dx + 2 \dot{\theta} \rho \int_0^L (b + x) \dot{y} dx \quad (7)$$

where  $\bar{I}$  is the total moment of inertia of the system, computed as

$$\bar{I} = I_3 + 2\rho \int_0^L (x + b)^2 dx \quad (8)$$

It should be noted that higher order terms in Eq. (7) were neglected, since it is assumed that the deformation of the appendage is small.

The total potential energy of the system under Euler- Bernoulli assumption [21], is:

$$V = \int_0^L EI (y'')^2 dx \quad (9)$$

where  $EI$  is the uniform flexural rigidity of the appendage, and  $y''$  is the second partial derivative of  $y$  with respect to  $x$ . The lateral displacement of any point on the appendage can be described by the product of spatial functions (the mode shape), and harmonic time functions as follows:

$$y(x, t) = \sum_{i=1}^n q_i(t) \phi_i(x) \quad (10)$$

where  $\phi_i(x)$  is called the mode shape, and  $q_i(t)$  describes the modal generalized coordinate for the  $i$ -th mode, and  $n$  denotes the number of modes retained in the approximation. Considering Eq. (9), the substitution of Eqs. (7) and (9) into Eq. (1) leads to the equations of motion in the following matrix form:

$$\mathbf{M}\ddot{\mathbf{q}} + \mathbf{K}\mathbf{q} = \mathbf{G}u \quad (11.1)$$

where  $\mathbf{M}$  and  $\mathbf{K}$  are the so-called mass and stiffness matrices, respectively,  $\mathbf{G}$  is the control input distribution vector,  $\ddot{\mathbf{q}}$  is the second time derivative of generalized coordinates  $\mathbf{q}$ . These parameters can be partitioned as

$$\mathbf{M} = \begin{bmatrix} \mathbf{M}_{\theta\theta} & \mathbf{M}_{\theta q} \\ \mathbf{M}_{q\theta} & \mathbf{M}_{qq} \end{bmatrix} \quad \mathbf{K} = \begin{bmatrix} \mathbf{0} & \mathbf{0} \\ \mathbf{0} & \mathbf{K}_{qq} \end{bmatrix} \quad \mathbf{G} = \begin{bmatrix} 1 \\ \mathbf{0} \end{bmatrix} \quad (11.2)$$

where elements of the mass and stiffness matrices are obtained as

$$\mathbf{M}_{\theta\theta} = \bar{I} = I_3 + 2\rho \int_0^L (x+b)^2 dx \quad (12.1)$$

$$[M_{\theta q}]_i = [M_{q\theta}]_i^T = \rho \int_0^L (b+x)\phi_i(x) dx \quad (12.2)$$

$$[M_{qq}]_{ij} = \rho \int_0^L \phi_i(x)\phi_j(x) dx \quad (12.3)$$

$$[k_{qq}]_{ij} = \rho \int_0^L EI\phi_i'(x)\phi_j'(x) dx \quad (12.4)$$

where  $[\cdot]_i$  denotes the  $i$ -th element of the vector  $[\cdot]$ , and  $[\cdot]_{ij}$  denotes the  $(i, j)$  element of the matrix  $[\cdot]$ . The mode shape function  $\phi_i(x)$  for the appendage (fixed-free beam with length  $L$ ) is obtained as [21]:

$$\phi(x) = (\cosh k_i x - \cos k_i x) - \alpha_i (\sinh k_i x - \sin k_i x) \quad (13.1)$$

$$\alpha_i = \frac{\sinh k_i L - \sin k_i L}{\cosh k_i L + \cos k_i L} \quad (13.2)$$

The boundary conditions are considered as

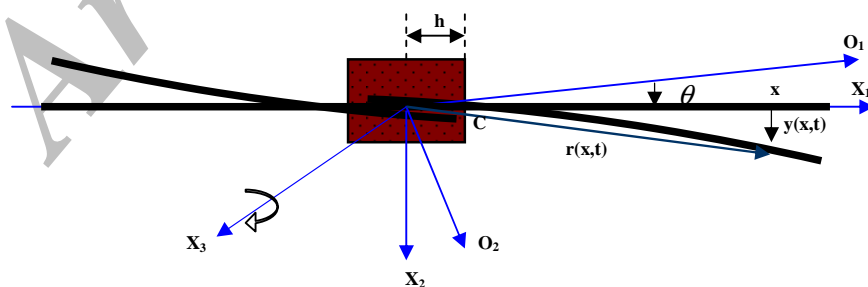


Fig. 1. Spacecraft configuration

$$\phi(0) = \phi'(0) = \phi''(L) = \phi'''(L) = 0 \quad (14)$$

The dynamics model of Eqs. (11) for a flexible spacecraft in a slewing maneuver is a suitable model for control analysis, [22], which is discussed next.

### 3. OPTIMAL CONTROL DESIGN

Considering the system dynamics described by a set of linear, undamped, ordinary differential equations such as Eqs. (11), the control torque  $u(t)$  is a scalar control input which is normally bounded as:

$$-u_{\max} \leq u(t) \leq u_{\max} \quad (15)$$

The system described by Eqs. (11) can be transformed into the decoupled modal equations using the eigenvalues and corresponding eigenvectors information of the system:

$$\ddot{\eta}_i + \omega_i^2 \eta_i = \Phi_i u \quad i = 1, \dots, n \quad (16)$$

where  $\eta_i(t)$  is the  $i$ -th modal coordinate,  $\omega_i$  is the  $i$ -th modal frequency ( $i$ -th diagonal element of eigenvalue matrix), and scalars  $\Phi_i$  are defined as

$$\Phi = [\Phi_1 \quad \Phi_2 \quad \dots \quad \Phi_n]^T = \Lambda G \quad (17)$$

where  $\Lambda$  is an  $n \times n$  matrix with its columns being the corresponding eigenvectors, and  $n$  is the number of modes considered in the control design. Eq. (16) can then be written in the following matrix form:

$$\ddot{\eta} + \Lambda \eta = \Phi u \quad (18.1)$$

Where

$$\Phi^T \mathbf{M} \Phi = I \quad , \quad \Phi^T \mathbf{K} \Phi = \Lambda \quad , \quad q = \Phi \eta \quad (18.2)$$

It is desired to convey the system described by Eqs. (18) from the initial conditions of  $\eta(0) = [0 \ 0 \ 0 \ \dots \ 0]^T$ , to the final conditions of  $\eta(t_f) = [\theta_f \ 0 \ 0 \ \dots \ 0]^T$  subjected to the input constraints (15) in *minimum time*, where  $\theta_f$  is the final angular position of the spacecraft in the slewing maneuver. Therefore, the performance index for the optimal law will be as follows:

$$J = \int_0^{t_f} dt = t_f \quad (19)$$

where the initial time is taken as zero and  $t_f$  is the given time for the maneuver. The rigid-body mode can be described by the first equation of Eqs. (18). In this case,  $\omega_1 = 0$  and so we obtain

$$\ddot{\eta}_1 = \Phi_1 u \quad \text{which can be transform to } \rightarrow \ddot{\theta} = \Phi_1 u \quad (20.1)$$

The boundary conditions are

$$\begin{aligned} \theta(0) = \dot{\theta}(0) = \dot{\theta}(t_f) &= 0 \\ \theta(t_f) &\equiv \theta_f \end{aligned} \quad (20.2)$$

Now, writing a state-space model for Eq. (20) yields

$$\begin{aligned} \dot{x}_1 &= x_2 \\ \dot{x}_2 &= \Phi_1 u \end{aligned} \quad (21)$$

where  $x_1 = \theta$  and  $x_2 = \dot{\theta}$  are the angular displacement and velocity of the space platform, respectively. To implement methods developed in the optimal control theory, [22], based on the performance index described by Eq. (19) and the dynamic equations as described by Eqs. (21), the system Hamiltonian is defined as

$$H = t_f + \lambda_1 \dot{x}_1 + \lambda_2 \dot{x}_2 = t_f + \lambda_1 x_2 + \lambda_2 \Phi_1 u \quad (22)$$

where  $\lambda_1$  and  $\lambda_2$  are the *costate variables* (or Lagrange multipliers). Using Pontryagin's minimum principle to characterize the optimal solution, the optimal control input is obtained as follows:

$$u_1(t) = u_{\max} [1(t) - 2[1(t - t_1)] + 1(t - t_f)] \quad (23)$$

where  $1(t)$  is the unit step function, and  $u_1(t)$  describes the well-known bang-bang solution function, [22]. The control profile is characterized with a single switching time  $t_1$ . If this control input is applied to the system as described by Eqs. (11), its vibration will be inevitable due to neglecting the flexible modes. To eliminate this oscillating motion, one should eliminate the sharp transitions of the bang-bang input so that the energy transfer to the flexible modes is minimized. This is discussed in the next section.

#### 4. REALISTIC OPTIMAL CONTROL DESIGN

In this section, the control input profile given by Eq. (23) is approximated by a smooth and continuous profile throughout the entire maneuver, with the saturation limits of  $\pm u_{\max}$ . Furthermore, this will reflect practical limitations in exerting bang-bang actuator forces/torques in reality, due to delays and non-zero time constants of existing actuation elements. Therefore, a realistic optimal (near-minimum time) control law is found that eliminates the jump-discontinuities of the input torque in order to reduce structural vibrations. By this near-optimal approach, we can "tune" the control profile in such a way that it systematically trades off residual vibration with the maneuver time. To this end, the time derivative constraints of the control input can be used. In the following, two cases are considered as employing the first and second derivatives for reshaping the control input profile.

**Case I. First derivative constraint of control input.** The bang-bang input obtained in the previous section is shown in Fig. (2a). An approximated control input that is smoother than the bang-bang input is shown in Fig. (2b). This control input is obtained by adding another state variable to the first time optimal control problem which describes the first time derivative of the control input, along with an additional constraint that confines the magnitude of this derivative to a given value. Consequently, the degree of smoothness of the generated control input is controlled by choosing an appropriate value for the maximum value of the input first time derivative, [19]. Considering the new Hamiltonian for the three state variables, and using Pontryagin's minimum principle, as will be discussed in the next section, the modified control input is obtained as

$$u_2(t) = a u_{\max} \sum_{j=0}^5 b_{1j} (t - t_j) 1(t - t_j) \quad (24)$$

where  $b_1 = [1, -1, -1, 1, 1, -1]$ ,  $1(t - t_j)$  defines the unit step function,  $t_0 = 0$ ,  $t_5 = t_f$ , and "a" is the slope of the inclined lines which is the maximum value of the input first time rate, and controls the smoothness of the modified input  $u_2(t)$ . The rate of this control input is shown in Fig. (3a), which certainly satisfies the given limits.

**Case II. Second derivative constraint of control input.** To make the control input smoother than the one computed in the previous case, one could add a fourth state variable to the previous time optimal control problem which describes the second time derivative of control input, along with an additional constraint that confines the magnitude of the second rate to a given value Fig. (2c). Following a similar procedure as described above, the modified control input in this case is obtained as

$$u_3 = \frac{a' u_{\max}}{2} \sum_{j=0}^{10} b_{2j} (t - t_j)^2 1(t - t_j) \quad (25)$$

where  $b_2 = [1, -1, -1, 1, 1, -1, -1, 1, 1, -1]$ ,  $1(t - t_j)$  defines the unit step function,  $t_0 = 0$ ,  $t_{10} = t_f$ , and "a'" is the maximum value of the input second time rate. The second rate of  $u_3(t)$  is shown in Fig. (3b).

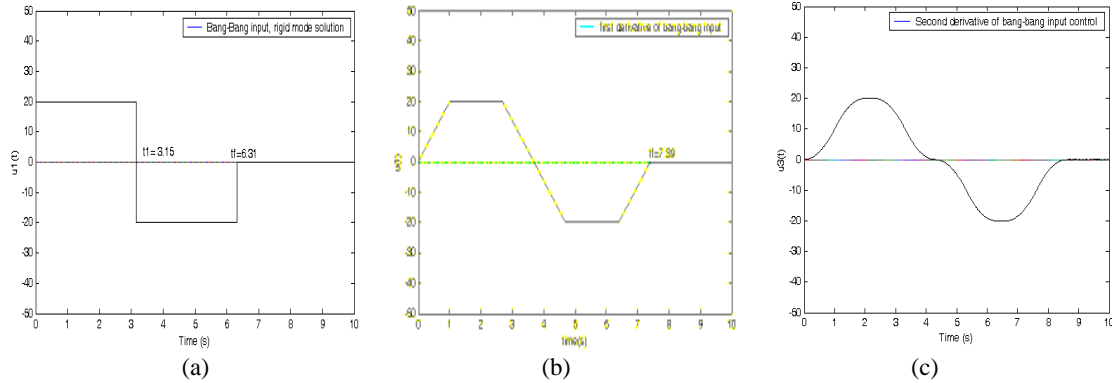
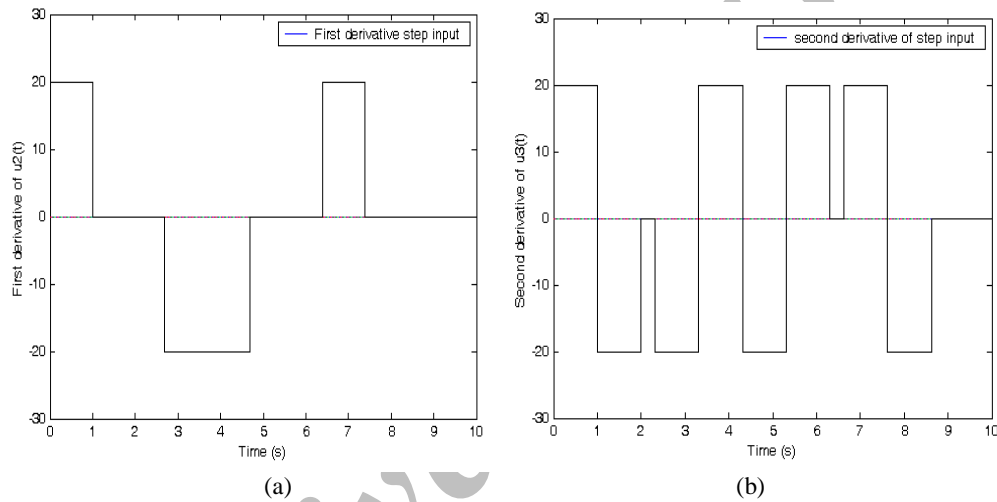


Fig. 2. Control input profile: a) Bang-Bang, b) Case I, c) Case II

Fig. 3. Control input derivatives: a) First rate of  $u_2(t)$ , b) Second rate of  $u_3(t)$ 

## 5. PARAMETER OPTIMIZATION PROCEDURE

In the previous section, the two modified control inputs,  $u_2$  and  $u_3$ , were obtained by reshaping the main bang-bang optimal control input profile. In each case, there are corresponding boundary conditions that construct boundary-value problems. The performance index for all cases is the one described by Eq. (19). The general constraints for all cases are as follows:

$$f_1 = x_1(t_f) - \theta_f = 0 \quad (26.1)$$

$$f_2 = x_2(t_f) = 0 \quad (26.2)$$

$$f_3 = u(t_f) = 0 \quad (26.3)$$

Those for  $u_2(t)$  are

$$f_4 = u_2(t_1) - u_{\max} = 0 \quad (26.4)$$

$$f_5 = u_2(t_3) + u_{\max} = 0 \quad (26.5)$$

and those for  $u_3(t)$  are

$$f_6 = u_3(t_2) - u_{\max} = 0 \quad (26.6)$$

$$f_7 = u_3(t_5) + u_{\max} = 0 \quad (26.7)$$

Then, the system Hamiltonian is introduced as

$$H = t_f + \sum \lambda_i f_i \quad (27)$$

where  $\lambda_i$  is the Lagrange multiplier for the  $i$ -th constraint equation,  $f_i$ . By solving the following equations:

$$g_i = \frac{\partial H}{\partial \lambda_i} = 0 \quad i = 1, \dots, n_i \quad (28.1)$$

$$g_j = \frac{\partial H}{\partial t_j} = 0 \quad j = 1, \dots, n_j \quad (28.2)$$

where  $n_i$  and  $n_j$  are the number of constraints and switching times, respectively. Therefore, a set of  $n_i + n_j$  equations is obtained which can be solved to determine the switching times including the final maneuver time  $t_f$ , and the Lagrange multipliers. To solve the established set of equations various numerical techniques can be used. In this work, the simple shooting (Newton) numerical method is employed.

**Solution procedure.** The steps of the numerical procedure for the solution of the developed time optimal and near-minimum-time optimal control laws are summarized below.

- 1) Find the bang-bang control input profile for the first mode (rigid body mode) using Eq. (23).
- 2) To smoothen the bang-bang control profile, choose either case I or II, whichever makes a smooth transition between its steps in the form of an inclined line or a curve of order two, respectively.
- 3) Determine the constraints of the problem by considering the state equations and then convert the optimal control problem into the parameter optimization problem as discussed above.
- 4) Solve the parameter optimization problem by the shooting (Newton) method.

Next, the developed control law is applied on a given satellite during a slewing maneuver, and the simulation results are discussed.

## 6. SIMULATION RESULTS

To illustrate the numerical procedure, the slewing maneuver of a given satellite is considered. The system parameters and maneuver specifications are listed in Table 1. The flexible solar panels are considered as Euler-Bernoulli beams and simulated by the assumed modes method, in which the first five modes are retained in the dynamics model. A single torque actuator located on the main body (satellite bus) is used to control the rotating maneuver. The natural frequencies  $\omega_i$ , and the components of  $\Phi$  in Eq. (17), for the first five modes, are given in Table 2.

Now, to define  $u_1(t)$ , following the solution procedure the mid-maneuver and final times are obtained as  $t_1=3.155$ s and  $t_f=6.311$ s. The attitude of the rigid platform and the appendages are illustrated in Fig. (4). If we apply this control torque to the first flexible mode (second equation of Eqs. (16)), its response is obtained as shown in Fig. (5a). As shown in this figure, the amplitude of this vibration is about 10 cm and may cause drastic damage. To alleviate this vibrating motion, the control input  $u_2(t)$  is calculated and applied.



Table 1. System parameters and maneuver specifications

Parameter		Value
Distance between O and C	b	0.80 m
Central body inertia	$I_1$	132 Kg $m^2$
	$I_2$	77 Kg $m^2$
	$I_3$	135 Kg $m^2$
Solar panels length	L	4m
Solar panels thickness	t	0.02 m
Solar panels width	w	0.50 m
Solar panels material stiffness	EI	20.10 Nm $^2$
Solar panels material density	$\rho$	0.81 Kg/m $^2$
Maximum torque available	u	20 N.m
Total mass of spacecraft	M	800 Kg
Total slewing angle	$\theta_f$	20 deg

Table 2. Flexible modes specifications

I	$\omega_i$ (rad/s)	$\Phi_i$
1	0	0.0628
2	1.2355	-0.0328
3	6.9311	0.0092
4	19.3320	0.0043
5	38.2100	-0.0026

Following the presented solution procedure, switching times and the final maneuver time can be calculated as

$$t_1 = 1.0, t_2 = 2.69, t_3 = 4.694, t_4 = 6.389, t_f = 7.689s$$

The attitude of the rigid platform and the appendages are illustrated in Fig. (4). Solving for the first flexible mode, the vibration of the endpoint of the appendages are shown in Fig. (5b). Compared to that of  $u_1(t)$ , the amplitude has reduced by 2 cm. For more reduction one can increase the value of "a" which is taken equal to one so far, but this results in a trade off between the maneuver time and the amplitude of the vibration. The application of  $u_3(t)$  is a better approach for vibration suppression and maintaining the maneuver time near its minimum value. To this end, switching times and final maneuver time are obtained as

$$t_1 = 1.0, t_2 = 2.0, t_3 = 2.31, t_4 = 3.31, t_5 = 4.31 s$$

$$t_6 = 5.31, t_7 = 6.31, t_8 = 6.62, t_9 = 7.62, t_f = 8.62 s$$

The attitude of the rigid platform and the appendages are illustrated in Fig. (4), and the vibration of the endpoint of appendages are shown in Fig. (5c). As seen, the amplitude has reduced to 5.3 cm, which shows a drastic suppression of the endpoint vibration under the application of  $u_3(t)$ . Comparing the maneuver duration in these cases, it can be seen that the application of  $u_3(t)$  results in a 2.309s increase of maneuver time (where  $t_f=6.311s$  is the minimum duration obtained for  $u_1(t)$ ), while reducing the amplitude of appendage vibration by 55%.

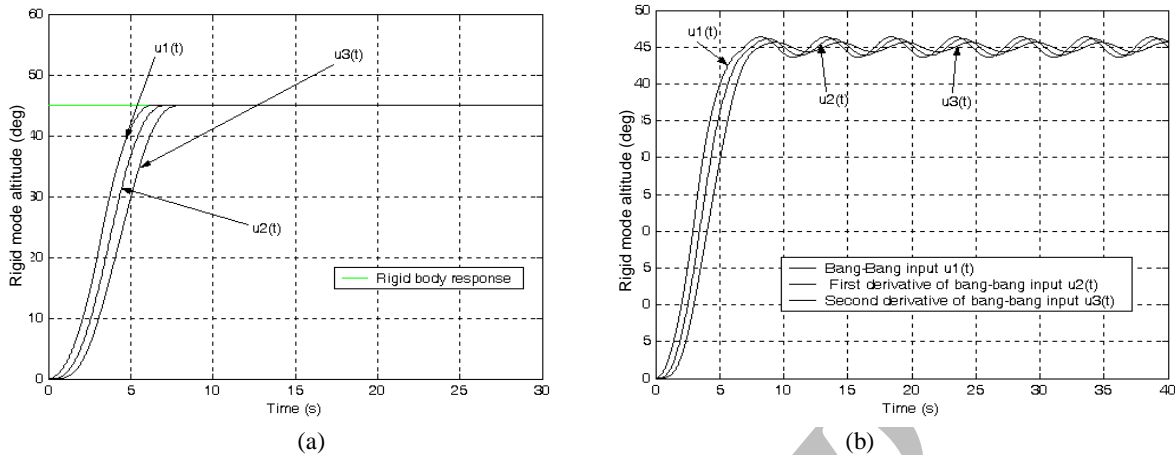


Fig. 4. Attitude response to three inputs: a) Rigid body, b) Appendages.

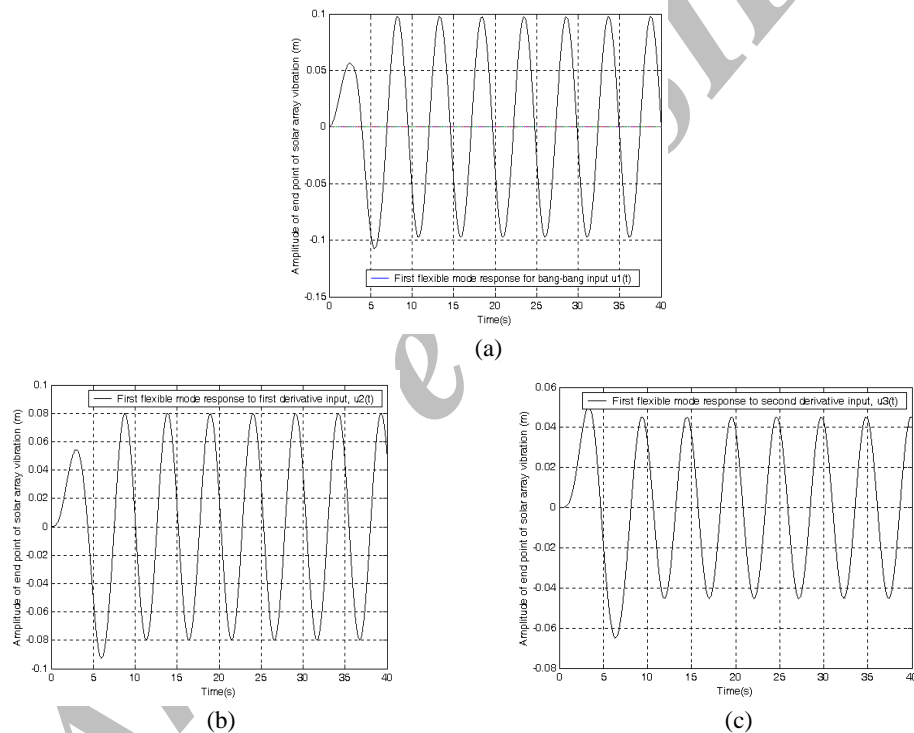


Fig. 5. First flexible mode response to: a) Bang-Bang, b) Case I, c) Case II

## 7. CONCLUSION

In this paper, a near-minimum-time optimal control law for a rigid space platform with flexible links during an orientating maneuver with a large angle of rotation was developed. The time optimal control solution for the rigid-body mode was obtained as a bang-bang function, and applied to the flexible system after smoothing the control inputs to reflect practical limitations in exerting bang-bang actuator forces/torques. The modified control input was obtained by adding additional state variables to the original time optimal control problem to describe the derivatives of control input, along with additional constraints that confine the magnitude of the derivatives to the given values. The developed control law was applied on a given satellite (called Sepehr) consisting of two elastic panels during a slewing maneuver. The simulation results revealed that the developed near optimal input compared to the bang-

bang solution goes well with the practical limitations and alleviates the vibration of the flexible appendages.

### REFERENCES

1. Ollero, A., Morel, G., Bernus, P., Nof, S. Y., Sasiadek, J., Boverie, S., Erbe, H. & Goodall, R. (2002). Milestone report of the manufacturing and instrumentation coordinating committee: From MEMS to enterprise systems. *Annual Reviews in Control*, Vol. 26, No. 2, pp. 151-162.
2. Jacobsen, S., Lee, C., Zhu, C. & Dubowsky, S. (2002). Planning of safe kinematic trajectories for free flying robots approaching an uncontrolled spinning satellite. *Proc. Of ASME 2002 Design Engineering Technical Conferences*, Montreal, Canada.
3. Vafa, Z. & Dubowsky, S. (1987). On the dynamics of manipulators in space using the virtual manipulator approach. *Proc. of IEEE Int. Conf. on Robotics and Automation*, pp. 579-585.
4. Moosavian, S. A. A. & Papadopoulos, E. (1998). On the kinematics of multiple manipulator space free-flyers and their computation. *Journal of Robotic Systems*, Vol. 15, No. 4, pp. 207-216.
5. Moosavian, S. A. A. & Papadopoulos, E. (2004). Explicit dynamics of space free-flyers with multiple manipulators via spacemapl. *Journal of Advanced Robotics*, Vol. 18, No. 2, pp. 223-244.
6. Cyril, X., Angeles, J. & Misra, A. (1991). Dynamics of flexible multibody mechanical systems. *Transactions of the CSME*, Vol. 15, No. 3, pp. 235-256.
7. Mah, H. W., Modi, V. J., Morita, Y. & Yokota, H. (1990). Dynamics during slewing and translational maneuvers of the space station based MRMS. *Journal of the Astronautical Space Sciences*, Vol. 38, No. 4, pp. 557-579.
8. Kuang, J. L., Kim, B. J., Lee, H. W. & Sung, D. K. (1998). The attitude stability analysis of a rigid body with multi-elastic appendages and multi-liquid-filled cavities using the chateau method. *Journal of the Astronautical Space Sciences*, Vol. 15, No. 1, pp. 209-220.
9. Papadopoulos, E. & Moosavian, S. A. A. (1994). Dynamics & control of multi-arm space robots during chase & capture operations. *Proc. Of IEEE/RSJ Int. Conf. on Intelligent Robots and Systems (IROS)*, Munich, Germany.
10. Moosavian, S. A. A. & Rastegari, R. (2002). Disturbance rejection analysis of multiple impedance control for space free-flying robots. *Proc. Of the IEEE/RSJ Int. Conf. on Intelligent Robots and Systems (IROS)*, Switzerland.
11. Ebrahimi, A., Moosavian, S. A. A. & Mirshams, M. (2004). Minimum-time optimal control of flexible spacecraft for rotational maneuvering. *Proc. Of IEEE Int. Conf. on Control Applications*, Taipei, Taiwan.
12. Ebrahimi, A., Moosavian, S. A. A. & Mirshams, M. (2005). Robust optimal control of flexible spacecraft during slewing maneuvers. *Journal of Aerospace Science and Technology*, Vol. 2, No. 4, pp. 39-45.
13. Moosavian, S. A. A., Rastegari, R. & Papadopoulos, E. (2005). Multiple impedance control for space free-flying robots. *AIAA Journal of Guidance, Control, and Dynamics*, Vol. 28, No. 5, pp. 939-947.
14. Moosavian, S. A. A. & Rastegari, R. (2006). Multiple-arm space free-flying robots for manipulating objects with force tracking restrictions. *Journal of Robotics and Autonomous Systems*, Vol. 54, No. 10, pp. 779-788.
15. Barbieri, E. & Ozgunar, U. (1993). A new minimum-time control law for a one- mode model of a flexible slewing structure. *IEEE Transactions on Automatic Control*, Vol. 38, No. 1, pp. 142-146.
16. Singh, G., Kabamba, P. T. & McClamroch, N. H. (1989). Planar, time-optimal, rest-to-rest slewing maneuvers of flexible spacecraft. *Journal of Guidance, Control and Dynamics*, Vol. 12, No. 1, pp. 71-81.
17. Bobrow, J. E., Dubowsky, S. & Gibson, J. S. (1985). Time-optimal control of robotic manipulators along specified paths. *The International Journal of Robotics Research*, Vol. 4, No. 3, pp. 244-258.

18. Byers, R. M., Vadali, S. & Junkins, J. L. (1990). Near minimum time, closed loop slewing of flexible spacecraft. *Journal of Guidance, Control, and Dynamics*, Vol. 13, No.1, pp. 57-65.
19. Albassam, B. A. (2002). Optimal near- minimum- time control design for flexible structures. *Journal of Guidance Control, and Dynamics*, Vol. 25, No. 4, pp. 618-625.
20. Junkins, J. L. & Kim, Y. (1993). *Introduction to dynamics and control of flexible structures*. AIAA Education Series.
21. Meirovitch, L. (1968). *Elements of vibration analysis*. McGraw- Hill Company.
22. Bryson, A. E. Jr. & Ho, Y. C. (1975). *Applied optimal control*. Hemisphere, Washington DC.

Archive of SID